

REPORT DOCUMENTATION PAGE			Form Approved OMB NO. 0704-0188	
<p>The public reporting burden for this collection of information is estimated to average 1 hour per response, including the time for reviewing instructions, searching existing data sources, gathering and maintaining the data needed, and completing and reviewing the collection of information. Send comments regarding this burden estimate or any other aspect of this collection of information, including suggestions for reducing this burden, to Washington Headquarters Services, Directorate for Information Operations and Reports, 1215 Jefferson Davis Highway, Suite 1204, Arlington VA, 22202-4302. Respondents should be aware that notwithstanding any other provision of law, no person shall be subject to any penalty for failing to comply with a collection of information if it does not display a currently valid OMB control number.</p> <p>PLEASE DO NOT RETURN YOUR FORM TO THE ABOVE ADDRESS.</p>				
1. REPORT DATE (DD-MM-YYYY)		2. REPORT TYPE		3. DATES COVERED (From - To)
		New Reprint		-
4. TITLE AND SUBTITLE			5a. CONTRACT NUMBER	
Role of Geometry on the Color of Flux Noise in dc SQUIDS			W911NF-09-1-0351	
			5b. GRANT NUMBER	
			5c. PROGRAM ELEMENT NUMBER	
			411359	
6. AUTHORS			5d. PROJECT NUMBER	
F. C. Wellstood, C. Urbina, John Clarke				
			5e. TASK NUMBER	
			5f. WORK UNIT NUMBER	
7. PERFORMING ORGANIZATION NAMES AND ADDRESSES			8. PERFORMING ORGANIZATION REPORT NUMBER	
University of Maryland - College Park Research Admin. & Advancement University of Maryland College Park, MD 20742 -5141				
9. SPONSORING/MONITORING AGENCY NAME(S) AND ADDRESS(ES)			10. SPONSOR/MONITOR'S ACRONYM(S) ARO	
U.S. Army Research Office P.O. Box 12211 Research Triangle Park, NC 27709-2211			11. SPONSOR/MONITOR'S REPORT NUMBER(S)	
			56204-PH-CSQ.4	
12. DISTRIBUTION AVAILABILITY STATEMENT				
Approved for public release; distribution is unlimited.				
13. SUPPLEMENTARY NOTES				
The views, opinions and/or findings contained in this report are those of the author(s) and should not be construed as an official Department of the Army position, policy or decision, unless so designated by other documentation.				
14. ABSTRACT				
<p>We examine the behavior of low frequency flux noise measured in ten Nb-NbOx-PbIn dc SQUIDS in the temperature range 1 K to 20 mK. As previously reported, the flux noise power spectrum <math>S(f)</math> typically scales with frequency as <math>A/f^2</math>. Remarkably, the excess noise power <math>A</math> at 1 Hz increases as the temperature is decreased below about 0.7 K, saturating to a value around <math>(10^{??})^2/\text{Hz}</math> below about 0.2 K. Here we report on the dependence of both the magnitude <math>A</math> and the slope <math>??</math> on the size and linewidth of the SQUID loops. In particular, at</p>				
15. SUBJECT TERMS				
Flux noise, SQUIDS, two-level systems, 1/f noise				
16. SECURITY CLASSIFICATION OF:			17. LIMITATION OF ABSTRACT	15. NUMBER OF PAGES
a. REPORT	b. ABSTRACT	c. THIS PAGE	UU	19a. NAME OF RESPONSIBLE PERSON
UU	UU	UU	UU	Chris Lobb
				19b. TELEPHONE NUMBER
				301-405-6130

## Report Title

Role of Geometry on the Color of Flux Noise in dc SQUIDs

### ABSTRACT

We examine the behavior of low frequency flux noise measured in ten Nb-NbO<sub>x</sub>-PbIn dc SQUIDs in the temperature range 1 K to 20 mK. As previously reported, the flux noise power spectrum  $S(f)$  typically scales with frequency as  $A/f^\alpha$ . Remarkably, the excess noise power  $A$  at 1 Hz increases as the temperature is decreased below about 0.7 K, saturating to a value around  $(10^{-20})^2/\text{Hz}$  below about 0.2 K. Here we report on the dependence of both the magnitude  $A$  and the slope  $\alpha$  on the size and linewidth of the SQUID loops. In particular, at the lowest temperatures we find that  $\alpha$  declines to values as low as 0.5 in the smallest devices, while  $\alpha$  is in the range 0.9–1 for the largest devices.



---

**REPORT DOCUMENTATION PAGE (SF298)**  
**(Continuation Sheet)**

---

Continuation for Block 13

ARO Report Number 56204.4-PH-CSQ  
Role of Geometry on the Color of Flux Noise in d ...

Block 13: Supplementary Note

© 2011 . Published in IEEE Transactions on Applied Superconductivity, Vol. 21, (3), Ed. 0 (2011), (Ed. ). DoD Components reserve a royalty-free, nonexclusive and irrevocable right to reproduce, publish, or otherwise use the work for Federal purposes, and to authorize others to do so (DODGARS §32.36). The views, opinions and/or findings contained in this report are those of the author(s) and should not be construed as an official Department of the Army position, policy or decision, unless so designated by other documentation.

Approved for public release; distribution is unlimited.

# Role of Geometry on the Color of Flux Noise in dc SQUIDS

F. C. Wellstood, C. Urbina, and John Clarke

**Abstract**—We examine the behavior of low frequency flux noise measured in ten Nb – NbO<sub>x</sub> – PbIn dc SQUIDS in the temperature range 1 K to 20 mK. As previously reported, the flux noise power spectrum  $S_{\Phi}(f)$  typically scales with frequency as  $A/f^{\alpha}$ . Remarkably, the excess noise power  $A$  at 1 Hz increases as the temperature is decreased below about 0.7 K, saturating to a value around  $(10 \mu\Phi_0)^2/\text{Hz}$  below about 0.2 K. Here we report on the dependence of both the magnitude  $A$  and the slope  $\alpha$  on the size and linewidth of the SQUID loops. In particular, at the lowest temperatures we find that  $\alpha$  declines to values as low as 0.5 in the smallest devices, while  $\alpha$  is in the range 0.9–1 for the largest devices.

**Index Terms**—Flux noise, SQUIDS, two-level systems,  $1/f$  noise.

## I. INTRODUCTION

RECENT measurements on flux qubits reveal the presence of excess low-frequency flux noise that causes dephasing when the device is biased away from the “sweet-spot” [1]. This flux noise appears to be of the same type as that first reported more than 20 years ago in a number of thin-film dc SQUIDS that were cooled below 1 K [2], [3]. The spectral density  $S_{\Phi}(f)$  of this noise was found to be of the form  $A/f^{\alpha}$ , where  $f$  is the frequency and  $\alpha$  typically lies between 0.5 and 1.0. Furthermore,  $A$  increased rather slowly with the dimensions of the SQUIDS. Only recently—with the impetus of research into quantum computing—has significant new theoretical and experimental work been undertaken to identify the underlying cause of the noise. A consensus has been developed that the noise is due to randomly flipping electronic spins distributed in a thin layer on the metallic surfaces of the devices [4]–[13]. Theoretical investigations [4], [9], [12] showed that this picture is consistent with the slow scaling of the noise power with SQUID dimensions.

Manuscript received August 03, 2010; accepted November 03, 2010. Date of publication December 23, 2010; date of current version May 27, 2011. This work was supported by the Director, Office of Science, Office of Basic Energy Sciences, Materials Science and Engineering Division of the US Department of Energy under Contract #DE-AC03-76SF00098, by the Center for Nanophysics and Advanced Materials (CNAM), the Laboratory for Physical Sciences (FCW), and by the Office of the Director of National Intelligence (ODNI), Intelligence Advanced Research Projects Activity (IARPA), through the Army Research Office.

F. C. Wellstood is with the Joint Quantum Institute and CNAM, Department of Physics, University of Maryland, College Park, MD 20742 USA (e-mail: well@umd.edu).

C. Urbina is with the Quantronics Group, SPEC-CEA-Saclay, 91191 Gif-sur-Yvette CEDEX, France (e-mail: cristian.urbina@cea.fr).

J. Clarke is with the Department of Physics, University of California. He is also with the Materials Sciences Division, Lawrence Berkeley National Laboratory, Berkeley, CA 94720 USA (e-mail: jclarke@berkeley.edu).

Color versions of one or more of the figures in this paper are available online at <http://ieeexplore.ieee.org>.

Digital Object Identifier 10.1109/TASC.2010.2093092

In particular [9], [12], it was shown that  $S_{\Phi}(f)$  scales as  $d/w$  in the limit  $w/d \ll 1$ , where  $d$  is the outer dimension of the SQUID and  $w$  is the linewidth of the SQUID loop. This scaling was confirmed experimentally by Lanting *et al.* [13].

Despite this progress, many unusual features of the noise remain unexplained or poorly understood. Here, we examine additional results from our early study [2] not previously published that highlight some of the most puzzling features of flux noise, in particular the unusual dependence of the exponent  $\alpha$  on the temperature and geometry of the device. In Section II we describe the SQUIDS that we studied, and in Section III briefly describe our measurement technique. We present our experimental results in Section IV, and in Section V discuss them in terms of a loss tangent. We describe the temperature and geometry dependence of  $\alpha$  in Section VI, and present our conclusions in Section VII.

Drung *et al.* [14] reported similar variations in  $\alpha$  at the same Applied Superconductivity Conference.

## II. SQUID GEOMETRY AND PARAMETERS

To understand how the flux noise varies with the SQUID layout, we fabricated dc SQUIDS with a variety of sizes and geometries. Figs. 1 and 2 show the layout of the larger and smaller SQUIDS, respectively. The SQUIDS were fabricated on oxidized Si wafers (except for devices K1 and J1 which were on a sapphire wafer) using photolithographic patterning. First, a 35-nm thick AuCu resistive shunt layer was evaporated and patterned with liftoff. This was followed by a 200-nm thick sputtered Nb layer which was patterned in an SF<sub>6</sub>+O<sub>2</sub> plasma etch. Two SiO insulation layers (500-nm total thickness), were evaporated, using a 1–2 nm underlayer of Cr or Ti as an adhesion promoter, and  $2 \times 2 (\mu\text{m})^2$  windows for the tunnel junctions were opened using liftoff. The counter-electrode layer was patterned in resist and the wafer scribed into chips.

The tunnel junctions were formed by placing a chip in a diffusion-pumped vacuum chamber and ion-milling the exposed Nb electrode for 40 s to remove surface oxide. The chamber was vented, and the chip was removed and remounted in an rf Ar – O<sub>2</sub> plasma oxidation chamber to produce NbO<sub>x</sub> on the cleaned Nb electrode. The chamber was re-evacuated and a 200-nm layer of Pb+5%In evaporated to form the junction counter-electrodes, which were patterned with lift-off in acetone.

Table I gives the parameters for ten devices. The loop inductance  $L$  was estimated from the measured modulation depth of the current  $I$  versus flux  $\Phi$ ; this introduced some spread in the values, even for devices with identical geometry. For example, although D1, D2, M1, and M2 have the same loop geometry,

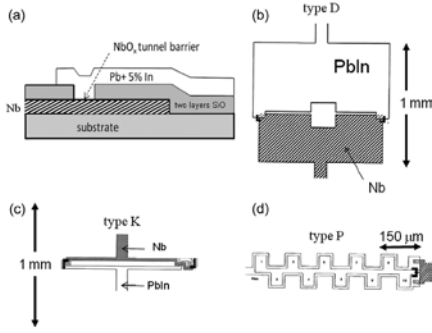


Fig. 1. (a) Side-view of layer structure used in the SQUIDs. A thin AuCu layer is deposited on a substrate and patterned to form shunts (not shown). This is followed by a Nb layer and two insulating layers of SiO<sub>2</sub> that define two  $2 \mu\text{m} \times 2 \mu\text{m}$  windows. A NbO<sub>x</sub> tunnel barrier is grown on the Nb and the top layer of Pb + 5% In is added to complete the Nb – NbO<sub>x</sub> – PbIn tunnel junctions. (b)-(d) Configuration of larger SQUIDs: Types D, K, and P. Type M SQUIDs have the same layout as type D, except for the addition of large area AuCu cooling fins to the shunts [15].

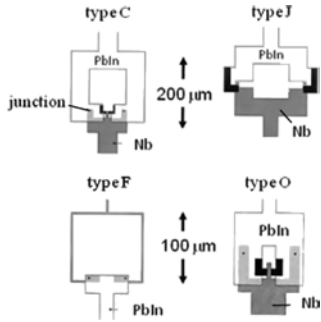


Fig. 2. Configuration of smaller SQUIDs: Types C, F, J and O. Junction and layer descriptions same as in Fig. 1.

their estimated loop inductances range from 440 pH to 515 pH with an average of 480 pH.

### III. EXPERIMENTAL ARRANGEMENTS

The low-frequency magnetic flux noise signal from a dc SQUID is small. To measure this noise we connected the device under test (SQUID 1) in series with a small resistor  $R_x \sim 0.07 \Omega$ , an rf-choke ( $L_{rf} \sim 12 \mu\text{H}$ ) and the input coil  $L_i$  of a second dc SQUID acting as a noise detector (Fig. 3). SQUID 2 was a Nb square washer design with 1 mm outside dimension, a  $180 \mu\text{m}$  inner hole dimension and an integrated input coil with 20 turns (except for that used for measuring device M2 which had 50 turns). This SQUID was operated in a flux-locked loop (FLL) [16], a current source  $I_{b1}$  was connected across  $R_x$ , and a second current source  $I_{\Phi_1}$  was used to apply flux to SQUID 1.

For a given applied flux  $\Phi_1$ , SQUID 1 was voltage biased by applying current  $I_{b1}$  greater than its critical current. Changes in flux in SQUID 1 change the current  $I_1$  passing through it and  $L_i$ , causing the flux  $\Phi_2$  in SQUID 2 to change and ultimately producing a change in the output voltage  $V_{out}$  from the FLL. The arrangement allows us to measure the noise in SQUID 1 as well as its current-voltage ( $I_1 - V_1$ ) and current-flux ( $I_1 - \Phi_1$ ) characteristics.

To obtain the power spectral density of the system noise at specific  $I_1 - \Phi_1$  bias points for SQUID 1, we connected the

TABLE I  
DEVICE PARAMETERS

#	L	$2I_0$	d	w	$\ell$	$A_p$	$\sqrt{A}$	$\alpha$
	(pH)	( $\mu\text{A}$ )	( $\mu\text{m}$ )	( $\mu\text{m}$ )	( $\mu\text{m}$ )	( $\mu\text{m}^2$ )	$\frac{\mu\Phi_0}{\sqrt{Hz}}$	
D1	440	6.3	1000	300-550	2200	$2 \times 10^5$	14.5	0.96
D2	500	4.5	1000	300-550	2200	$2 \times 10^5$	14.5	0.95
M1	515	5.6	1000	300-550	2200	$2 \times 10^5$	18	0.94
M2	470	6.2	1000	300-550	2200	$2 \times 10^5$	14	0.92
P1	1500	1.77	144-740	10	2560	$5 \times 10^4$	14.5	0.74
K1	530	11.4	75-1000	20	1700	$7 \times 10^4$	11	0.72
J1	200	21.6	200	50	560	$2 \times 10^4$	5	0.71
F1	700	5.7	100	2	390	$1 \times 10^4$	8	0.67
O1	45	1.36	90-105	36	120	$2 \times 10^3$	7	0.60
C2	210	5.3	200	50	400	$2 \times 10^4$	7.5	0.50

SQUID parameters listed in descending order of the slope  $\alpha$ . First column gives the device name. L is the loop inductance,  $2I_0$  is the maximum critical current (for nominally zero flux bias), d is the outside dimension of the SQUID loop (two dimensions are given for non-square loops), w is the linewidth of the SQUID loop,  $\ell$  is the approximate length around the inner hole of the SQUID loop, and  $A_p$  is the approximate pick-up area of the loop.  $\sqrt{A}$  is the square root of the excess flux noise power spectral density at 1 Hz and  $\alpha$  is the noise slope, both taken at the lowest temperature measured for the device.

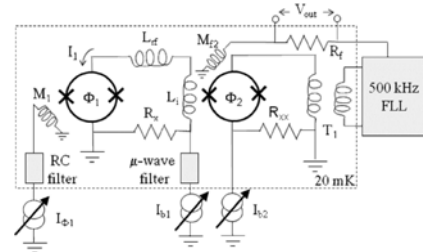


Fig. 3. Flux noise in SQUID 1 is measured by SQUID 2 operated in a flux-locked loop. SQUID 1 is voltage-biased by  $R_x = 0.07 \Omega$  and current source  $I_{b1}$  so that changes in the flux  $\Phi_1$  in SQUID 1 lead to changes in the current  $I_1$  through SQUID 1. Changes in  $V_{out}$  from the FLL are proportional to changes in flux in SQUID 2, which in turn are proportional to changes in  $I_1$ .

voltage output of the flux-locked loop to a spectrum analyser. From the slope of the  $I_1 - \Phi_1$  curve at the bias point, this noise power spectrum is readily transformed into an effective flux noise in SQUID 1 (Fig. 4).

The measured and measurement SQUIDs were enclosed in separate compartments in a Nb tube mounted in a sealed Cu cell. The cell was bolted to the mixing chamber of a dilution refrigerator and filled with superfluid helium for good thermal contact. To reduce the ambient magnetic field, external magnetic noise and rf-interference, the dewar was surrounded with two mu-metal cylinders and the entire experiment was installed in a Cu-mesh rf-shielded room. We made noise measurements from 4.2 to 0.02 K, with SQUID 1 biased to a few  $\mu\text{V}$  (power  $\sim 0.1 \text{ nW}$ ).

### IV. FLUX NOISE SPECTRAL DENSITY VERSUS TEMPERATURE

Fig. 4 shows two typical flux noise power spectra. Ignoring noise peaks at 60 and 180 Hz, the spectra obey

$$S_{\Phi}(f) = A f^{-\alpha} + C, \quad (1)$$

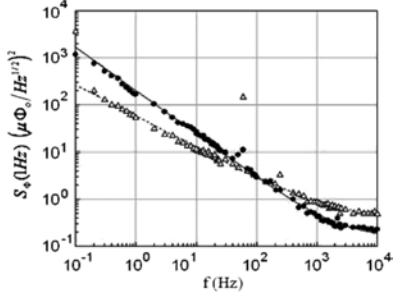


Fig. 4. Power spectral density of magnetic flux noise  $S_{\Phi}$  versus frequency  $f$  for SQUID F1 (open triangles) at  $T = 0.14$  K and M2 (closed circles) at  $T = 0.021$  K. Dashed curve is fit to white noise plus  $1/f^{\alpha}$  noise with  $\alpha = 0.67$  for F1 and solid curve is similar fit for M2 with  $\alpha = 0.92$ .

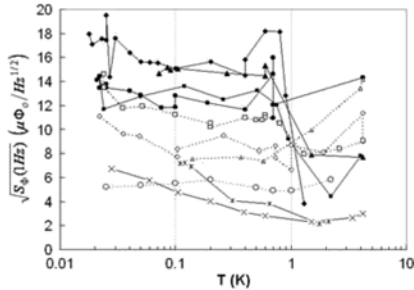


Fig. 5. Magnitude of magnetic flux noise at 1 Hz versus temperature  $T$ . The symbols are for devices D2 ■, M1 ◆, D1 ▲, M2 ●, P1 □, K1 ◇, J1 ○, F1 ×, O1 △, and C2 \*.

where  $A$  is a constant,  $C$  is frequency-independent (white) noise from the device under test and measuring system, and  $\alpha$  is the slope of the excess noise on a log-log plot. In analogy with white noise, noise with  $\alpha$  near 1 is called “pink noise” because there is more noise at lower (“red”) frequencies. As Fig. 4 shows, the noise in SQUID M2 is more “red” than that in F1.

Fig. 5 shows the square root of the flux noise power spectrum at 1 Hz plotted versus temperature  $T$  for the 10 devices listed in Table I. For  $T > 1$  K, the noise may contain significant contributions from critical current noise [17], but this falls rapidly as the temperature decreases. Below 1 K the excess noise was dominated by a flux-like term, that is, the output noise scaled with the slope of the  $I_1 - \Phi_1$  curve, as expected for a fluctuating flux in the SQUID.

As noted previously, there are remarkable features in this behavior. (i) Broadly speaking, devices with similar geometry tend to produce similar noise. (ii) Ignoring the behavior above 1 K which contains significant critical current noise [17] and is material dependent [2], the noise tends to increase as  $T$  decreases from 1 K. (iii) The largest devices (D1, D2, M1, M2, bolder solid curves in Fig. 5) tend to have larger noise with a broad peak around 0.5 to 0.7 K. Smaller devices (for example, C2 and O1, thin solid curves in Fig. 5) have smaller noise, which tends not to change much with temperature below 1 K or increase steadily as  $T$  decreases. (iv) At the lowest temperatures the noise for all the devices falls in the range 5 to  $18 \mu\Phi_0/\text{Hz}^{1/2}$  at 1 Hz, despite the diverse range of device parameters (Table I): the inductances  $L$  range from 45–1500 pH, the critical currents range from 1–22  $\mu\text{A}$ , the pickup areas  $A_p$  of the SQUID loops vary

from about  $2 \times 10^3 (\mu\text{m})^2$  to  $2 \times 10^5 (\mu\text{m})^2$ , and the linewidths of the films used to make the SQUID loops vary from 2  $\mu\text{m}$  to 300  $\mu\text{m}$  or greater. In addition, devices (J1 and K1) made on a sapphire substrate also exhibit similar noise, and the fraction of the loop made from Nb or PbIn does not seem to affect the noise level. These general observations are consistent with measurements on other devices, embracing a wider range of parameters, including measurements by Yoshihara *et al.* [1] on much smaller aluminum flux qubits [ $A_p \sim 2 (\mu\text{m})^2$ ] with somewhat smaller estimated levels of noise ( $1\text{--}2 \mu\Phi_0/\text{Hz}^{1/2}$  at 1 Hz). As mentioned earlier, the relatively slow dependence of the noise amplitude on the SQUID dimensions can be explained in terms of fluctuating electron spins distributed uniformly on the surface [4], [9], [12].

## V. MAGNETIC LOSS TANGENT

The existence of spin fluctuations must be accompanied by dissipation. For a magnetic material, we can characterize the dissipation in terms of the magnetic loss tangent,  $\tan(\mu_m)$ , the ratio of the imaginary part of the magnetic susceptibility to the real part. Applying the fluctuation-dissipation theorem to a material with a magnetic loss tangent yields:

$$\tan(\delta_m) \approx S_{\Phi}(f)/2k_B T L \eta. \quad (2)$$

The filling factor  $\eta$  accounts for the distribution of material around the SQUID loop:  $\eta = 1$  for a uniform 3D distribution.

Eq. (2) implies that  $\tan(\mu_m)$  is independent of frequency if the noise scales as  $1/f$  and that loops with the same filling factor will exhibit a noise power spectrum that scales with the loop inductance. We can view  $\tan(\mu_m)$  as a figure of merit that accounts for expected effects of the loop and source geometry. Here, as the distribution of the sources is unknown, we set  $\eta = 1$  to find an effective  $\tan(\mu_m)$ .

Fig. 6 is a plot of the effective  $\tan(\mu_m)$  at 1 Hz versus temperature  $T$  for the noise data shown in Fig. 5. Overall, the magnitude is rather low, but increases significantly as the temperature decreases. Fig. 6 shows that at any temperature the loss tangent of the devices falls within a band that spans an order of magnitude. While both Figs. 5 and 6 show a spread of an order of magnitude, note that Fig. 5 is a plot of the square root of the power spectral density, while  $\tan(\mu_m)$  is proportional to the power. Although further analysis of the filling factor is needed, this behavior implies that the noise power scales approximately with loop inductance  $L$ . Thus, the noise energy  $S_{\Phi}(f)/2L$  is roughly constant at a given temperature.

## VI. SLOPE OF FLUX NOISE VERSUS TEMPERATURE

Fig. 7 shows a plot of the slope  $\alpha$  of the  $1/f^{\alpha}$  flux noise versus temperature  $T$  for the 10 devices. The values of  $\alpha$  at the lowest temperatures are also listed in Table I. The four largest devices (D1, D2, M1, M2) all show  $\alpha \sim 1$  at 0.5 K, slowly decreasing with temperature  $T$  to about  $\alpha \sim 0.9$  at 20 mK, while above 0.7 K  $\alpha$  falls rapidly as  $T$  increases.

In contrast, the smaller devices show  $\alpha$  markedly lower than 1 below 1 K. Despite large differences in shape and dimensions, devices J1, F1, K1 and P1 behave quite similarly:  $\alpha \sim 0.8$  at 0.5 K, decreasing to 0.7 below 100 mK. Device C2 shows

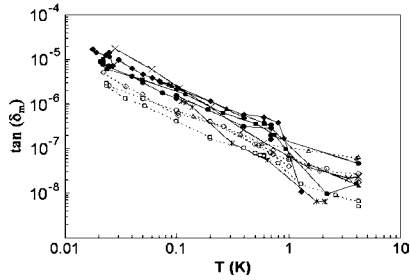


Fig. 6. Effective magnetic loss tangent  $\tan(\delta_m)$  at 1 Hz versus temperature  $T$  for data shown in Fig. 5. The symbols are for devices D2 ■, M1 ◆, D1 ▲, M2 ●, P1 ○, K1 □, J1 ◇, F1 ◊, O1 ⊕, and C2 ✱.

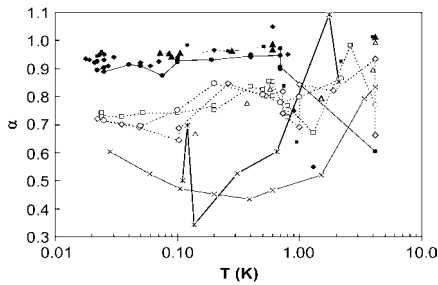


Fig. 7. Slope  $\alpha$  of the  $1/f^\alpha$  flux noise versus temperature for 10 devices. The symbols are for devices D2 ■, M1 ◆, D1 ▲, M2 ●, P1 ○, K1 □, J1 ◇, F1 ◊, O1 ⊕, and C2 ✱.

a singular behavior, with considerable variation around 0.1 K. The device with the smallest center hole (O1) showed a consistently low slope, reaching a minimum of about 0.45 at 0.4 K, and increasing to  $\sim 0.6$  at 30 mK. We note that while F1 has the smallest loop linewidth ( $2 \mu\text{m}$ ) and an intermediate sized center hole ( $390 \mu\text{m}$ ) it behaves more like devices J1, K1 and P1 than the device with the smallest center hole (O1). This suggests that the inner length of the loop may be an important factor in determining the slope of the noise. As one sees from Table I, however, an overriding distinction may be that D1, D2, M1, M2 with  $\alpha \geq 0.92$  all have large linewidths ( $w \geq 300 \mu\text{m}$ ) while the remaining devices with  $\alpha \leq 0.74$  have relatively narrow linewidths ( $w \geq 50 \mu\text{m}$ ).

## VII. CONCLUSION

In conclusion, we measured  $1/f^\alpha$  flux noise in ten Nb – NbO<sub>x</sub> – PbIn dc SQUIDS below 1 K and found a strong dependence of the slope  $\alpha$  on temperature and SQUID geometry. Smaller SQUIDS—with narrower linewidths—showed markedly lower values of  $\alpha$  and a different dependence on temperature than larger SQUIDS—with wider linewidths. These results are inconsistent with a random distribution of *uncorrelated* noise sources [7], which would cause the noise magnitude but not the slope to vary with geometry, and suggests that there is a spatial correlation to the flux noise. Indeed, correlations among spins are predicted to produce values of  $\alpha$  that can be well below unity [11]. We note that none of our devices showed the flattening of the  $1/f$  noise at frequencies below

$f_w$  predicted by the spin-diffusion model [9]. These authors suggest, however, that weakly coupled spins further away from the superconductor and the presence of strongly coupled spin pairs could produce noise with nonzero slope at frequencies below  $f_w$ .

Our measurements were carried out long before the development of microscopic models of the  $1/f$  flux noise [4], [6], [9], [10], [11]. Lacking insight from these models, we did not systematically vary only  $d$  and  $w$ , the key parameters in the models [9], [12], as was done, for example, in [13]. Thus, we cannot usefully compare the noise magnitude of our own devices with predictions [4], [9], [12]. Future measurements should be carried out with SQUIDS in which only a single parameter is varied to determine whether  $\alpha$  depends on, for example, linewidth or hole size.

## ACKNOWLEDGMENT

FCW thanks L. Faoro, L. Ioffe, S. Lloyd, R. McDermott and R. Schoelkopf for useful discussions on flux noise.

## REFERENCES

- [1] F. Yoshihara *et al.*, “Decoherence of flux qubits due to  $1/f$  flux noise,” *Phys. Rev. Lett.*, vol. 97, pp. 167001-1–167001-4, Oct. 2006.
- [2] F. C. Wellstood, “Excess Noise in the dc SQUID: 4 K to 20 mK,” Ph.D. dissertation, Dept. of Physics, University of California Berkeley, 1988.
- [3] F. C. Wellstood, C. Urbina, and J. Clarke, “Low frequency noise in dc superconducting quantum interference devices below 1 K,” *Appl. Phys. Lett.*, vol. 50, pp. 772–774, Jan. 1987.
- [4] R. H. Koch, D. P. DiVincenzo, and J. Clarke, “Model for  $1/f$  flux noise in SQUIDS and qubits,” *Phys. Rev. Lett.*, vol. 98, pp. 267003-1–267003-4, June 2007.
- [5] S. Sendelbach *et al.*, “Magnetism in SQUIDS at Millikelvin temperatures,” *Phys. Rev. Lett.*, vol. 100, pp. 227006-1–227006-4, June 2008.
- [6] S.-K. Choi *et al.*, “Localization of metal-induced gap states at the metal-insulator interface,” *Phys. Rev. Lett.*, vol. 103, pp. 197001-1–197001-4, Nov. 2009.
- [7] S. Sendelbach, D. Hover, M. Mück, and R. McDermott, “Complex inductance, excess noise, and surface magnetism in dc SQUIDS,” *Phys. Rev. Lett.*, vol. 103, pp. 117001-1–117001-4, Sept. 2009.
- [8] H. Bluhm *et al.*, “Spinlike susceptibility of metallic and insulating thin films at low temperatures,” *Phys. Rev. Lett.*, vol. 103, pp. 026805-1–026805-4, July 2009.
- [9] L. Faoro and L. B. Ioffe, “Microscopic origin of low-frequency flux noise in Josephson circuits,” *Phys. Rev. Lett.*, vol. 100, pp. 227005-1–227005-4, June 2008.
- [10] R. de Sousa, “Dangling-bond spin relaxation and magnetic  $1/f$  noise from the amorphous-semiconductor/oxide interface: Theory,” *Phys. Rev. B*, vol. 76, pp. 245306-1–245306-15, Dec. 2007.
- [11] Z. Chen and C. C. Yu, “Comparison of Ising spin glass noise to flux and inductance noise in SQUIDS,” *Phys. Rev. Lett.*, vol. 104, pp. 247204-1–247204-4, June 2010.
- [12] R. C. Bialczak *et al.*, “ $1/f$  flux noise in Josephson phase qubits,” *Phys. Rev. Lett.*, vol. 99, pp. 187006-1–187006-4, Nov. 2007.
- [13] T. Lanting *et al.*, “Geometrical dependence of the low-frequency noise in superconducting flux qubits,” *Phys. Rev. B*, vol. 79, pp. 060509-1–060509-4, Feb. 2009.
- [14] D. Drung *et al.*, “Investigation of low-frequency excess flux noise in dc SQUIDS at mK temperatures,” *IEEE Trans. Appl. Supercond.*, vol. 21, no. 3, June 2011.
- [15] F. C. Wellstood, C. Urbina, and J. Clarke, “Hot-electron effects in metals,” *Phys. Rev. B*, vol. 49, pp. 5942–5942, March 1994.
- [16] F. C. Wellstood, C. Heiden, and J. Clarke, “Integrated dc SQUID magnetometer with a high slew rate,” *Rev. Sci. Instr.*, vol. 55, pp. 952–957, 1984.
- [17] F. C. Wellstood, C. Urbina, and J. Clarke, “Flicker ( $1/f$ ) noise in the critical current of Josephson junctions at 0.09–4.2 K,” *Appl. Phys. Lett.*, vol. 85, pp. 5296–5298, Nov. 2004.